
Article:
Adiya, ZISG orcid.org/0000-0003-2247-3047, Dupont, V orcid.org/0000-0002-3750-0266 and Mahmud, T orcid.org/0000-0002-6502-907X (2019) Steam reforming of shale gas with nickel and calcium looping. Fuel, 237. pp. 142-151. ISSN 0016-2361

https://doi.org/10.1016/j.fuel.2018.09.092

Paper accepted 20 September 2018 in *Fuel*

Steam reforming of shale gas with Nickel and Calcium looping

Zainab Ibrahim S G Adiya, Valerie Dupont, Tariq Mahmud

School of Chemical and Process Engineering (SCAPE), The University of Leeds, Leeds LS2 9JT, UK

Keywords: Packed bed, CaO sorbent, chemical looping, Ni-based oxygen transfer material, Steam reforming, Hydrogen

Abstracts

High purity H_2 production from shale gas using sorption enhanced chemical looping steam reforming (SE-CLSR) was investigated at 1 bar, GHSV 0.498 hr^{-1}, feed molar steam to carbon ratio of 3 and 650 °C for 20 reduction-oxidation-calcination cycles using CaO and 18 wt. % NiO on Al_2O_3 as sorbent and catalyst/oxygen carrier (OC) respectively. The shale gas feedstock was able to cyclically reduce the oxygen carrier and subsequently reform with high H_2 yield and purity. For example H_2 yield of 31 wt. % of fuel feed and purity of 92 % were obtained in the 4^{th} cycle during the pre-breakthrough period (prior to cycles with low sorbent capacity). This was equivalent to 80 and 43 % enhancement compared to the conventional steam reforming process respectively.

1. Introduction

Hydrogen is regarded as the fuel of the future while worldwide demand for H_2 is expected to rise in both chemical and energy use [1]. Various processes for H_2 production such as partial oxidation, auto-thermal reforming, water electrolysis, biomass gasification and steam reforming have become commercially successful since it (H_2) was discovered by Henry Cavendish in 1788. Catalytic steam reforming (C-SR) has emerged as the major technology for syngas production (in large scale) [2-6] in refining and petrochemical complexes [7] and steam methane reforming has become the most common method for large scale H_2 production for years [8]. Despite having reached technological and

commercial maturity, the C-SR process is still one of the most energy intensive processes for syngas production through its heating requirement with high operational and maintenance cost [1, 9]. To generate high purity H_2 and maximise yield, additional units such as water-gas shift (WGS) and separation units (such pressure swing adsorption, membrane or cryogenic technology) are included in a C-SR plant [10-12], making the process complex and economical only at large scales [11]. Global warming is presently one of the major concern in the world [13, 14]. The C-SR process is also one of the contributors of global warming; by increasing the CO_2 concentration in the atmosphere. For every 4 mole of H_2 produced by complete steam methane reforming process for example, a mole of CO_2 is generated. In addition to tons of CO_2 generated [15] and release into the atmosphere by the reformer furnace flue gas. Thermodynamic constraints are also a major drawback of the process to date [16, 17] requiring the process to be operated at high temperature, whilst medium-high pressures (30-40 bar) which thermodynamically limit the fuel conversion, have to be used to reduce plant size. Other challenges of the process include risk of coke formation, limited catalyst effectiveness and overall the efficiency of the process has reached its maximum [18-20].

Researchers are presently focusing on novel technologies that generate H_2 at lower cost, eliminating or reducing the major remaining challenges with C-SR process. The development of technologies such as membrane reactor [21-25] permit C-SR reaction at mild operating conditions suppressing the thermodynamic limitations [10]. Similarly, coupling of C-SR with chemical looping usually termed Chemical looping steam reforming or 'CL-SR' [13, 26-30] can minimise energy requirement, and sorption enhanced steam reforming (SE-SR) [31-35], as well as sorption enhanced chemical looping steam reforming (SE-CLSR) [6, 36-42] combine H_2 production and CO_2 capture in a single reactor enhancing H_2 yield and purity compared to the conventional process, avoiding a separate water gas shift stage, and lowering the burden of H_2 separation. Membrane assisted SR, CLSR, SESR and SE-CLSR are all part of the current efforts in process intensification of H_2 production via reforming methods. The latter (SE-CLSR process) also minimises the energy requirement of operating the system to a great extent by close-coupling the heat demand of H_2 production with the heat released by the

chemisorption of its CO_2 by-product. Detail process description with schematics of the SE-SR and SE-CLSR process can be found in S G Adiya et al [9, 43] and Ryden and Ramos [39].

Hydrocarbons are the major feedstock in steam reforming process for the generation of H_2 and synthesis gas [44]. Approximately, 90 % of the global H_2 generated originates from conversion of fossil fuels [45]. A boom in shale gas production [13] and unconventional gas resources in the world such as hydrates foresees that gas will remain the main feedstock of steam reforming in the near term. The current development in oil and gas extraction such as drilling and fracking have made shale gas production economically viable [9]. Thus, additional techniques of gas consumption are also desirable due to its newfound albeit temporary abundance.

Presently, CaO is the best known natural solid high temperature CO_2 sorbent, and can be mined in the form of limestone ($CaCO_3$) and dolomite ($CaMg(CO_3)_2$). Because of the sorbent's low cost, significant CO_2 sorption/desorption capacity even after repeated cycles, and fast reaction kinetics, CaO as high temperature CO_2 sorbent has attracted much attention. CaO's theoretical capture capacity of CO_2 is as high as 0.786 g of CO_2/g of sorbent [46].

In the present study, experimental analysis of hydrogen production via the SE-SR and SE-CLSR processes using a model composition shale gas with $CaO_{(S)}$ sorbent and NiO based catalyst / oxygen carrier (OC) was conducted on a bench scale packed bed reactor for the first time. This follows from our previous study (S G Adiya el al [47]) which focused on the same materials and feedstock (NiO based catalyst / oxygen carrier (OC) and shale gas) and assessed via experiments the steam reforming of shale gas with and without chemical looping. The purpose of the study is to demonstrate the effect of coupling sorption enhacement (SE) and chemical looping (CL) in C-SR process in packed bed reactor using a realistic feedstock, as well as validate our previous thermodynamic equlibrium analysis in S G Adiya et al [9].

2. Materials and Methodology

2.1 Experimental Materials

The model shale gas mixture used for the experiment was reproduced from cylinders of different hydrocarbons. The desired molar composition (Table 1) was calculated based on the mole fraction of the species and a given total volumetric flow rate selected according to desired gas hourly space velocity (GHSV). A detailed description of the experimental materials and rig set-up can be found in the supplementary data (SD1 and SD2) and was described in a previous publication [47]. CaO sorbent and commercial 18 wt. % nickel oxide on aluminium oxide support (NiO on Al_2O_3 support) catalyst was provided by Twigg Scientific & Technical Ltd for the experimental study. The catalyst performed the dual action of catalyst and OC.

Table 1 Composition of shale gas used for experiments [48]

Species	Composition (%) [48]	Molar Flow (mol/s)
CH_4	79.4	2.68×10^{-6}
C_2H_6	16.1	5.44×10^{-7}
C_3H_8	4.0	1.35×10^{-7}
N_2	0.4	1.35×10^{-8}
Total	100	3.37×10^{-6}

2.2 Experimental procedure

2 g of catalyst and 1 g of CaO sorbent (1.2 mm mean size) were loaded into the reactor before setting up the experimental rig as described in SD2. The catalyst particle size was chosen to respect the particle-reactor diameter ratio (ca. 1/10) found in industrial SMR plants where diffusion as well as kinetic limitations control the reaction rates, while maintaining low pressure drop between reformer inlet and outlet and offering good mechanical strength. After setting the experimental rig, the furnace temperature was then set to the desired temperature e.g. 650 ℃. This was followed by reduction of the catalyst from non-active NiO to catalytically active Ni phase, conducted using a gas mixture feed of 5 vol. % hydrogen in nitrogen carrier gas. The nitrogen and hydrogen flow rate were 200 and 10 $cm^3\ min^{-1}$ (STP) respectively. Reduction of the NiO to Ni resulted in micro GC H_2 vol. % reading which remained at zero, and then returned to 5 vol. % after about 45 minutes, indicating that the catalyst had completed its reduction step. Hydrogen flow was then stopped, leaving only the nitrogen feed

until the hydrogen reading reached 0 % again, having flushed out all the reducing H_2 from the reactor. This was followed by the SE-SR process, which started by feeding water and fuel (shale gas) to the reactor using the programmable syringe and MKS flow controller respectively at the desired molar steam to carbon ratio. Experiments lasted for at least 3 hours and ended by turning off the water and fuel flows first, then the furnace. This left only nitrogen feed to completely flush out the reformate gases and cool down the reactor before turning off the chiller and dismantling the rig for the next experiments when the reactor temperature had reached ambient temperature.

The experimental procedure for the first cycle of SE-CLSR process was exactly the same as that of the SE-SR process procedure (above). In both processes an air feed of 500 cm^3 min^{-1} STP and 850 ℃ had the effect of simultaneously re-oxidising the catalyst/OC, and regenerating it by also burning off any carbon that might have deposited on the catalyst/OC. The choice of higher oxidation temperature of 850 ℃ was to fully regenerate the sorbent (CO_2 desorption by calcination). The recorded temperature during air feed increased by roughly 10-15 ℃ owing to the oxidations reactions of the carbon residue and re-oxidation of the nickel-based catalyst. The major difference between the experimental procedures of the SE-CLSR process and those of the SE-SR process was the presence of the reducing H_2/N_2 feed in the SE-SR process, whereas the SE-CLSR process relied on autoreduction of the catalyst.

The experimental procedure for C-SR process used for comparison was also exactly the same as that of the SE-SR process except that 3 g of catalyst on its own was used in the C-SR process as opposed to the 2 g of catalyst and 1 g of CaO in both the SE-SR and SE-CLSR processes. The choice of 2 g of catalyst in the SE- processes was a compromise between increasing the reactor bed load and increasing the gas input to maintain the same gas hourly space velocity when comparing the conditions with and without Ca sorbent. The latter, which resulted in a higher carbon input, was considered less logical. A full description of the post processing procedures allowing the calculations of water conversion, H_2 purity and molar yields of products can also be found in SD3. Explanation of thermodynamic methodology and characterisation techniques used can be found in SD4 and 5 respectively and are also described in [47].

3. Results and discussion

3.1 Sorption enhanced steam reforming (SE-SR) process of shale gas

3.1.1 Effect of temperature on SE-SR process

Temperature is one of the major variables on which the conversion of CaO and its carbonation capacity is determined. The effect of temperature on sorption enhanced steam reforming (SE-SR) process was investigated from 600 to 700℃ at GHSV 0.498, 1 bar pressure and feed molar steam to carbon ratio (S:C) of 3 using CaO as CO_2 sorbent. Higher temperature during sorption were not investigated as they owning to the thermal decomposition of $CaCO_{3(s)}$ [9, 49-51]. Moreover, the equilibrium vapour pressure of CO_2 over $CaO_{(S)}$ is low at low temperatures [9, 39, 52]. Consequently, only the range of 600 to 700℃ was investigated. Lower temperatures were not investigated either because they suppressed catalyst activity.

Table 2 presents the plots of average values of H_2 yield and purity over temperature range. H_2 yield and purity decreased gradually as temperature increased. This was expected because the SE process is favoured at low/medium temperature [38] for reasons explained earlier. The conversion of feedstocks (fuel and H_2O conversion) were not reported during the carbonation period because equations they are derived from were not applicable due to the inability to quantify the carbonation rate on the solid sorbent at any given time. However, gas yields including that of H_2 were quantifiable using the nitrogen balance.

Table 2 H_2 yield and purity in the pre-breakthrough period at 1 bar, GHSV 0.498 and S:C 3 using 18 wt. % NiO on Al_2O_3 support catalyst (average values)

Temperature ℃	H_2 yield (wt. % of fuel)	H_2 purity (%)
600	21.138	83.946
650	20.793	83.966
700	20.323	82.961

The effect of temperature (600-700 ℃) on the outlet gas composition in the SE-SR during the pre-breakthrough period (active sorbent stage or period before the sorbent starts saturating) is depicted in Table 3. In the pre-breakthrough period, the molar production rate of CO and CO_2 was completely

zero (at all the investigated temperature) owing to the presence of the sorbent (carbonation reaction and enhancement of water gas shift). CH_4 yield increased with increase in operating temperature. The low CH_4 yield in the low/medium temperature range was due to the shift in equilibrium caused by the CO_2 capture favouring the H_2 generation reactions and subsequently higher fuel conversion. The increase in the CH_4 yield with increasing temperature is no doubt caused by limited carbonation reaction and thermal decomposition of $CaCO_3$ which occurs at higher temperatures [49-51]. Hence, lowering the feed conversion as the sorption enhancement faded.

Table 3 Molar production rate of CH_4 and H_2 in the pre-breakthrough period at 1 bar, GHSV 0.498 and S:C 3 using 18 wt. % NiO on Al_2O_3 support catalyst (average values)

Temperature ℃	H_2	CH_4
600	6.82×10^{-6}	1.17×10^{-6}
650	6.71×10^{-6}	1.28×10^{-6}
700	6.55×10^{-6}	1.34×10^{-6}

In all the investigated temperatures, after the breakthrough period, CO and CO_2 generation commenced gently and stabilised at a certain point (roughly after about 3960 s of experiments) representing the emergence of the post breakthrough period as depicted in Figure 1. H_2 yield also decreased gently when moving from the breakthrough period to the post breakthrough period as depicted in Figure 1(a), almost degenerating the process back to the C-SR process levels. However, a comparison between the SE-SR and C-SR process will be made later.

The exothermic nature of the WGS reaction leads to a higher concentration of CO in both the breakthrough and post breakthrough period at higher temperatures. As for CO_2, sorbent saturation inhibits its removal to a certain extent by the exothermic carbonation reaction, thus the gradual increase in the CO_2 content of the product gas was observed as the process evolved from the breakthrough period to the post breakthrough period. During the breakthrough period, the molar production rate of CO_2 was primarily determined by the WGS reaction. At this point, less CO_2 was generated with increasing temperature owing to the suppression of the WGS reaction.

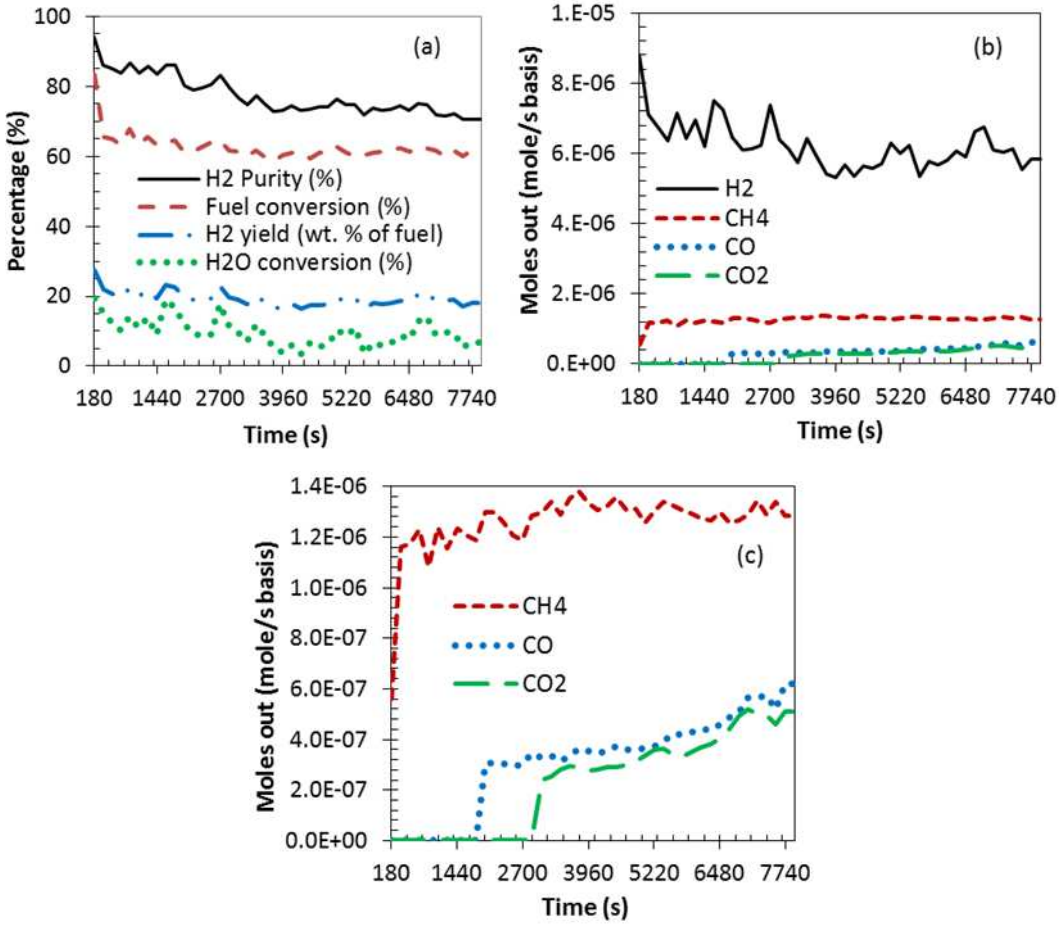

Figure 1 Process output vs time at 650 ℃ , 1 bar, GHSV 0.498 and S:C 3 using 18 wt. % NiO on Al_2O_3 support catalyst (a) H_2 yield and purity, fuel and H_2O conversion vs time (b) moles out vs time (c) clearer graph of moles out vs time

Numerous experimental researches have been done on the SE-SR process with varied feedstocks and sorbents. For example, Ding et al [53] examined the SE-SR process of CH_4 using hydrotalcite-based CO_2 adsorbent. Martavaltzi and Lemonidou [54] also investigation the SE-SR process using CH_4 and a new hybrid material NiO–CaO–$Ca_{12}Al_{14}O_{33}$ performing the dual action of both steam reforming catalyst and CO_2 sorbent. A direct comparison of the present study with previous work is not possible owing to the difference in the feedstock (shale gas). Nonetheless, most of the previous studies on the SE-SR process such as Zin et al and Esteban-Díez et al. [55, 56] including those mention earlier Ding et al and Martavaltzi and Lemonidou [53, 54] are in good agreement to those of the present studies with regards to substantially increased in H_2 yield and purity in the SE-SR compared to the C-SR process.

3.1.2 Comparison of SE-SR with C-SR and with chemical equilibrium

Figure 2 depicts a comparative analysis of the SE-SR and the C-SR process. As shown in the figures both H_2 yield and purity increased significantly in the presence of CaO sorbent compared to the Ca-free system. Up to 45 % and 46 % rise in H_2 yield and purity were achieved when the average process output of SE-SR was compared with that of the C-SR process at 600 ℃ under same operational condition (GHSV 0.498, 1 bar pressure and S:C 3). This is significantly higher than the C-SR process, despite the use of a lower mass of catalyst (2 g vs. 3 g).

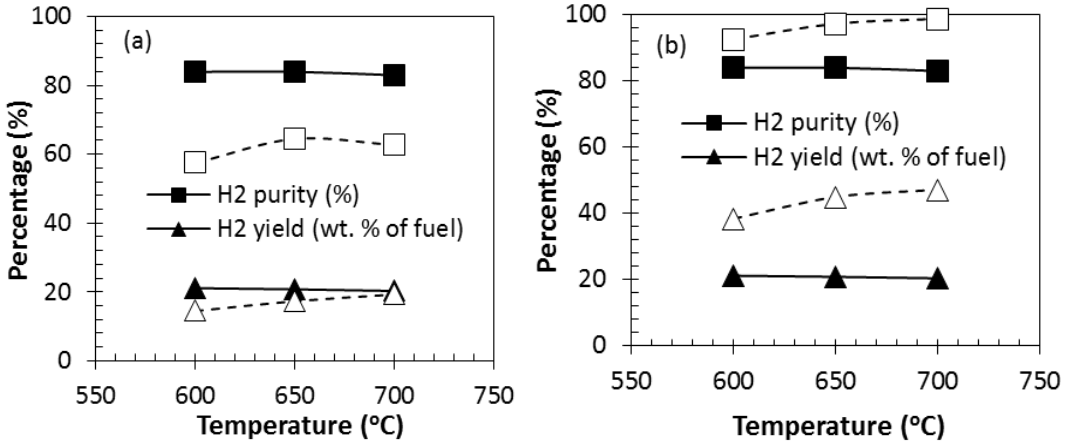

Figure 2 Comparison of SE-SR during the pre-breakthrough period with C-SR and chemical equilibrium results at 1 bar, GHSV 0.498 and S:C 3 using 18 wt. % NiO on Al_2O_3 support catalyst (a) comparison of SE-SR (solid lines with filled symbols) and C-SR process (dashed lines with unfilled symbols), H_2 yield and purity vs temperature (average values) (b) comparison of SE-SR (solid line with filled symbols) and chemical equilibrium (dashed lines with unfilled symbols), H_2 yield and purity vs temperature (average values)

The presence of sorbent in the system also lowered the temperature of maximum H_2 yield as depicted in Figure 2(a). To illustrate this, a comparison between the C-SR and SE-SR process optimum operating temperature can be used. The maximum H_2 yield and purity in the temperature range investigated (600-700 ℃) was at 700 ℃ for the C-SR process. This significantly dropped to 600 ℃ for the SE-SR process. The latter would significantly reduce the cost of operating the system and could permit the use of cheaper reactor materials afforded by the mild temperatures of the process unit.

The inability of the experimental results to reach equilibrium (Fig. 2b) could be attributed to mass transfer and kinetic limitations, and to loss of sorbent capacity over time. Kinetic limitations can be overcome by operating at higher temperature, whilst mass transfer limitations can be mitigated by reducing the particle size of the bed materials (catalyst/OC and sorbent) to such a size that there will

be no diffusion effect [45] and/or by decreasing the gas hourly space velocity, thus increasing the residence time of the reactions [47].

Comparing the results of the SE-SR process during the post breakthrough period with that of the conventional process leads to a surprising observation. It was expected that the SE-SR process will degenerate back to the C-SR process after the sorbent had become fully saturated (post breakthrough period). However, the opposite was observed. H_2 purity was higher in the SE-SR process even though the sorbent was saturated owing to a steady production of CO_2. Previous studies by Albrecht et al and Xie et al [34, 57] have reported a similar observation and attributed it to the fact that CO_2 is still absorbed by the sorbent during the post breakthrough period but very slowly. H_2 yield and fuel and water conversion were also higher at 600 ℃ in the SE-SR but merged (with insignificant difference) with the C-SR process at higher temperatures (650 and 700℃) as depicted in Figure 3. The phenomenon observed at 600 ℃ results from the fact that the carbonation reaction is favoured at low/medium temperatures while that of high temperatures (650 and 700℃) might result from the fact that the carbonation reaction is limited at higher temperatures [9] explained earlier. Table 4 presents percentage (%) enhancement of SE-SR process over the C-SR process (H_2 yield and purity). For a given parameter 'P' such as H_2 yield or H_2 purity, the percentage enhancement 'E_P' between SE-SR and C-SR is calculated as $E_P = ((P_{SE\text{-}SR} - P_{C\text{-}SR})/P_{C\text{-}SR}) \times 100$. Table 4 lists the values of $E_{H2\ yield}$ and $E_{H2\ purity}$ found in the experiments and those expected from equilibrium. The experimental results investigated at 600, 650 and 700 ℃ show 45, 19 and 5 % increase in H_2 yield and 46, 30 and 28 % increase in purity compared to the C-SR process. On the whole, the measured enhancing effects of sorption were stronger than those predicted between C-SR experiments and C-SR equilibrium states except for H_2 yield at 600 ℃ for equilibrium studies.

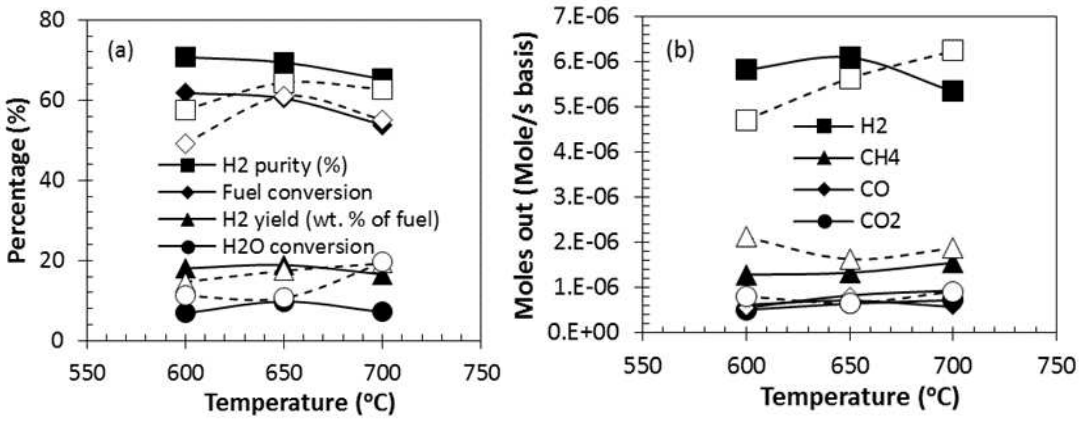

Figure 3 Comparison of SE-SR process during the post breakthrough period with C-SR process at 1 bar, GHSV 0.498 and S:C 3 using 18 wt. % NiO on Al_2O_3 support (a) average H_2 yield and purity, fuel and H_2O conversion (b) average outlet moles vs temperature (Note: Solid lines with filled symbols are SE-SR process results and dashed lines with unfilled symbols for C-SR process)

Table 4 Percentage (%) enhancement of SE-SR process over C-SR process ($E_{H2\ yield}$ and $E_{H2\ purity}$), comparison between values obtained in the experiments (Exp).

Operating Temperature	$E_{H2\ yield}$ (%), Exp	$E_{H2\ yield}$ (%), Eq.	$E_{H2\ purity}$ (%), Exp	$E_{H2\ purity}$ (%), Eq.
600 ℃	45	0	46	22
650 ℃	19	7	30	27
700 ℃	5	13	28	29

3.2 Sorption Enhanced Chemical looping steam reforming (SE-CLSR) process of shale gas

3.2.1 Effect of sorbent and chemical looping on steam reforming process

Reduction-oxidation-calcination cycles were conducted in the quartz fixed bed reactor. Again 2 g (1.2 mm mean sieve size) of the catalyst/OC was randomly mixed with 1 g (1.2 mm mean sieve size) of CaO sorbent and loaded in the reactor. For the purpose of studying the effect of sorption enhancement coupled with chemical looing in the C-SR process; the SE-CLSR experiments were performed at atmospheric pressure, GHSV 0.498, S:C ratio of 3 and a temperature of 650 ℃ under constant flow of inert N_2 gas. 20 reduction-oxidation-calcination cycles were conducted to investigate the cyclic behaviour and stability of the Ca based CaO sorbent and the 18 wt. % NiO on Al_2O_3 support catalyst/OC.

Figure 4 depicts the average process outputs (H_2 yield and purity) achieved in the 20 reduction-oxidation-calcination cycles. Fuel and water conversion during the pre-breakthrough period were excluded owing to the inability to accurately measure the carbonation rate on the solid sorbent at any given time explained earlier.

NiO reduction, steam reforming of shale gas and WGS reactions happen concurrently with in-situ CO_2 capture, causing substantial increase in H_2 yield and purity (compared to the C-SR process as depicted in Figure 4 as expected in the pre-breakthrough (active carbonation stage). The observed phenomenon results from the presence of the CO_2 sorbent shifting the equilibria of both the steam reforming and the WGS reaction to the right towards higher conversion to CO, then to CO_2, followed by capture of the CO_2 on the sorbent, with the carbon product becoming entirely solid calcium carbonate (during pre-breakthrough).

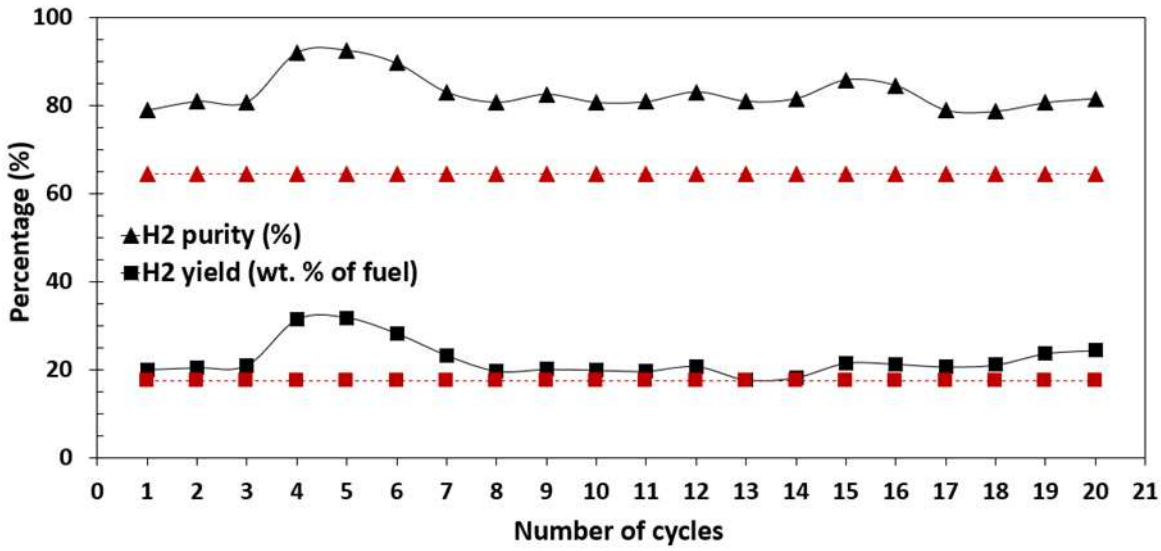

Figure 4 Comparison of SE-CLSR process outputs with C-SR at 1 bar, GHSV 0.498, S:C 3, reforming/reduction temperature at 650 ℃ and oxidation at 850 ℃ with CaO and NiO on Al_2O_3 support as sorbent and catalyst/OC respectively (pre breakthrough period average process outputs) (Note: Solid lines are for SE-CLSR and dashed lines for C-SR process)

Additionally, the presence of the nickel-based catalyst/OC in the SE-CLSR system also causes further positive effect on H_2 yield and purity, even though part of the fuel was initially used for reduction of the catalyst/OC. This is because the reduction of fuel by NiO produces total oxidation products CO_2

and H_2O, with the former being captured by the sorbent, and the latter increasing the water concentration of the system, effectively achieving a dual effect or enhancement in accordance with Le Chatelier's principle. The slight decrease in H_2 yield and purity after the 5th cycle, which fairly stabilises in the 8th cycle may be caused by a number of factors to be investigated, including loss of active sites of the catalyst/OC, which itself may arise from the accumulation of solid carbon by deposition on the surface of the catalyst/OC, extensive sintering of the Ni particles, and Ni active site blockage [47] , as well as loss of sorbent capacity over time, a well-known process for CaO sorbents undergoing cyclic carbonation-calcination at high temperatures and in the presence of steam. Comparison of the SE-CLSR process outputs with chemical equilibrium results is presented in Figure 5, the comparison shows that the SE-CLSR process experimental results were away from equilibrium for most cycles but were close to it for cycles 4, 5 and 6.

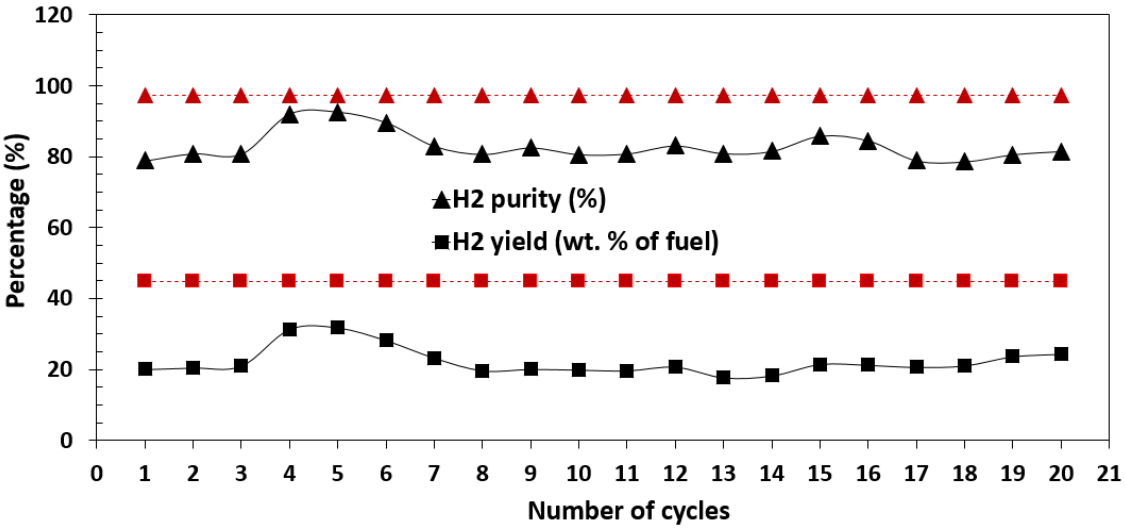

Figure 5 Comparison of SE-CLSR process outputs with chemical equilibrium results at 1 bar, GHSV 0.498, S:C 3, reforming/reduction temperature at 650 ℃ and oxidation at 850 ℃ with CaO and NiO on Al_2O_3 support as sorbent and catalyst/OC respectively (pre breakthrough period average process outputs) (Note: Solid lines are for SE-CLSR and dashed lines for chemical equilibrium results)

Figure 6 present the 4th cycle outputs against time stream chosen as best output representative of all the 20 reduction-oxidation-calcination cycles. The breakthrough period is followed by the post breakthrough period (CO_2 steady state production). At this stage the process is expected to degenerate back completely to the C-SR process owing to the full saturation of the Ca based CO_2

sorbent. Both H_2 yield and purity Figure 6(a) were higher during the pre-break through period with a gentle decline at the breakthrough period that approaches stability towards the post breakthrough period. However, it is worth remembering that, fuel and water conversion during the pre-breakthrough and breakthrough periods are not reliable for reasons explained earlier. The molar production rate of CO and CO_2 on the other hand increases with move from the breakthrough period to the post breakthrough period Figure 6(b).

During the oxidation stage conducted at 850 ℃, three major reactions were expected to happen. The regeneration of the sorbent, solid carbon oxidation reactions and nickel oxidation reaction. Both sorbent regeneration and carbon oxidation reactions have the potential to generate CO_2. The later (carbon oxidation reactions) and nickel oxidation reaction consumed oxygen from the air feed. Thus, carbon and oxygen elemental balances were not enough to define the three unknown rates of Ni oxidation, carbon oxidation, and sorbent calcination. Moreover, the most vital part of the oxidation reaction process is in the first 3 minutes, as the process is quite fast in the reactor. The micro gas chromatography analysed the results with a frequency of 3 minutes, rendering monitoring of the oxidation reaction process with time on stream impossible or unreliable with the micro-GC. However, an increase in the oxidation temperature was observed during the oxidation process due to the exothermic nature of the reaction. The burning off of the solid carbon (coke) deposition during the air feed was coincidental with CO_2 and CO generation. As the oxidation reaction approached its end, a gradual decrease in the reactor temperature was observed. SD6 presents a percentage enhancement of SE-CLSR process with C-SR process (H_2 yield and purity percentage).

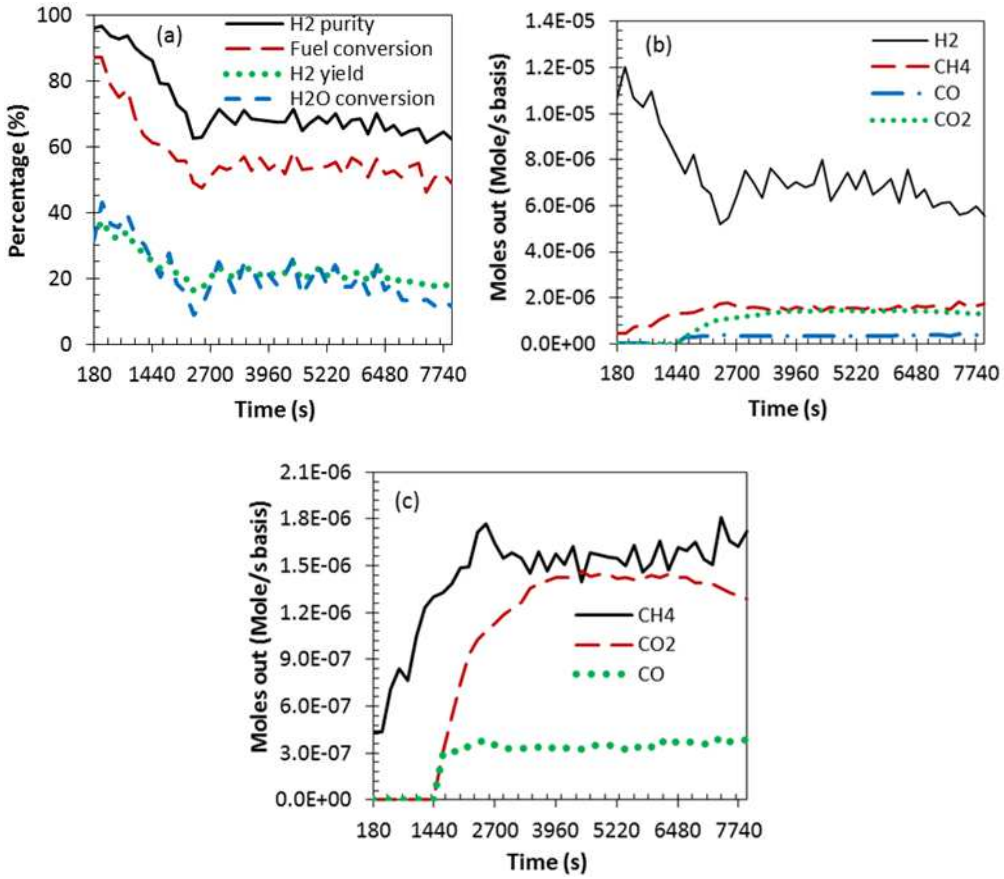

Figure 6 Process outputs for the 4th cycle at 1 bar, GHSV 0.498, S:C 3, reforming/reduction temperature at 650 ℃ and oxidation at 850 ℃ with CaO and NiO on Al_2O_3 support as sorbent and catalyst/OC respectively

Comparison of our results with previous research is difficult mainly because researchers focused on pure methane as feedstock, promoted Ca based CaO sorbent and a different catalyst/OC. For example, a similar study coupling sorption enhancement and chemical looping was conducted by Hafizi et al, [37] showing the application of $2Fe_2O_3/MgAl_2O_4$ and $22Fe_2O_3/Al_2O_3$ as catalyst/OC and cerium promoted CaO as CO_2 sorbent using pure methane as feedstock. Their characterisation findings and the SE-CLSR process experimental outputs shows the better performance of cerium promoted CaO sorbent for CO_2 removal. They also found that $2Fe_2O_3/MgAl_2O_4$ catalyst/OC exhibited better performance compared to $22Fe_2O_3/Al_2O_3$. The catalyst(s)/OC(s) and sorbent demonstrated stable performance at 600 ℃ in good nine reduction and calcination cycles. Antzara et al. [38] also investigated the performance of SE-CLSR process using a mixture of a bifunctional NiO-based catalyst/OC supported on ZrO_2, and a ZrO_2-promoted CaO-based CO_2 sorbent with pure methane as

feedstock. The materials showed excellent stability without deterioration in their performance for 20 continues reforming and regeneration cycles. They reported high H_2 concentration throughout the pre-breakthrough period with low concentration of CO and CO_2 which is in good agreement with the present study. Their conclusion that SE-CLSR process has significant advantages compared to the C-SR process is also in good agreement to that of the present study.

3.2.2 Comparison of SE-CLSR at post CO_2 breakthrough period with C-SR process

Comparison of the post breakthrough period of the SE-CLSR process and the C-SR process is shown in Figure 7, this presents a significant decrease in fuel and water conversion (which could be calculated since no CO_2 sorption was taking place), with resulting lower H_2 yield and purity in the SE-CLSR process at steady state of post CO_2 breakthrough in most of the cycles. This could be attributed to a number of factors. First, our catalyst bed was diluted with calcium carbonate, affecting the activity of the catalyst, although this effect was not observed for the uncycled, H_2 reduced SE-SR process. Most likely, another possible reason is the fact that there were potential deposits of carbon in both the catalyst and calcium carbonate beyond the 1 hour 30 minutes of use during the fuel/steam feed. The C-SR process experiments were conducted for a period of 1 hour 30 minutes while those of SE-CLSR process were conducted for a period of 3 hours to enable full observation of the pre-breakthrough period, breakthrough and the post pre-breakthrough period. This would have significantly affected both the fuel and water conversion, and subsequently the H_2 yield and purity.

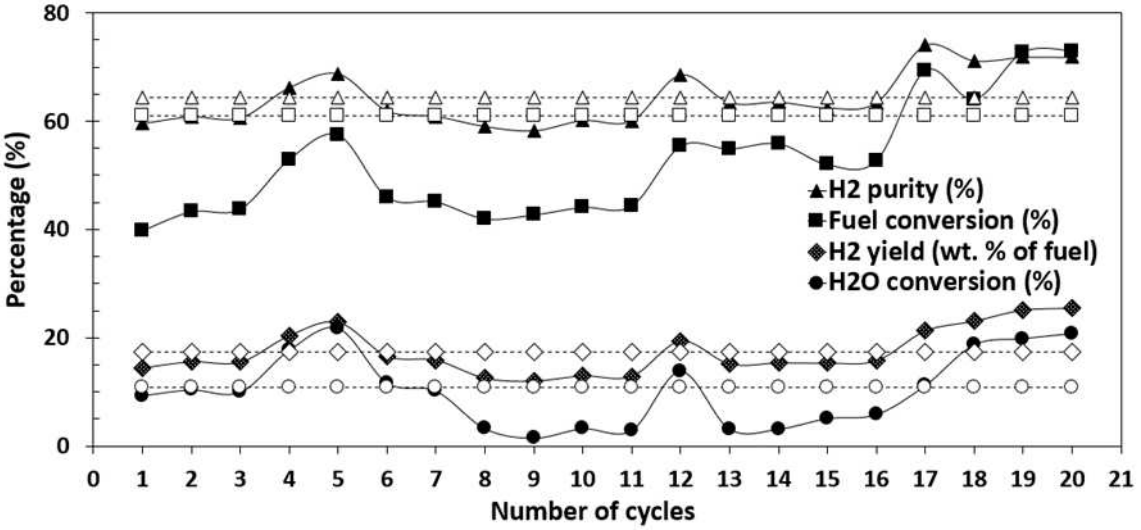

Figure 7 Comparison of post breakthrough period of SE-CLSR with the C-SR process at 1 bar, GHSV 0.498, S:C 3, reforming/reduction temperature at 650 ℃ and oxidation at 850 ℃ with CaO and NiO on Al_2O_3 support as sorbent and catalyst/OC respectively (Note: Solid lines are for experimental results and dashed lines for C-SR process)

3.3.3 Cyclic stability and behaviour of sorbent and catalyst/OC during SE-CLSR process

The stability of the CaO sorbent (from limestone) coupled with 18 wt. % Ni on Al_2O_3 support as catalyst/OC was determined by the increasing number of cycles and the carbonation efficiency of the sorbent. As seen in Figure 4; H_2 yield and purity increased at first steadily with increase in the number of cycles. At the 4^{th} cycle a significant rise in both the H_2 yield and purity was seen which was followed with a gentle decrease in both the yield and purity till approximately the 9^{th} cycle; where the process output almost stabilized (with insignificant difference). The later no doubt can be attributed to decrease in the sorbent capacity and loss of activity of the catalyst/OC with increasing usage. Even though CaO sorbents have many advantages as CO_2 sorbent, the sorbent's industrial application has faced some serious concerns including the loss of sorption capacity in long-term cyclic operation, and the formation of $CaSO_4$ owing to loss of reactivity with sulphur containing gases [46, 58-60]. Sintering of the sorbent, including agglomeration of particles, pore shape and shrinkage change are major causes of loss of CaO sorption capacity [46]. The gradual increase in the 1st cycle, might result from the fact that the reactivity NiO particles (catalyst/OC in the process) is known to increased slightly after first contact with fuel [39, 61].

Others researchers have studied the CO_2 sorption behavior of limestone sorbents in repeated cyclic absorption desorption cycles [46], for example, over 500 carbonation/calcination cycles were conducted by Grasa and Abanades [62], there results are in good agreement to those of the present study in the sense that sorbent capture capacity was significantly decreased during the first 20 cycles and then stabilized at a certain point limit.

4. Materials characterization after use

The X-ray diffraction patterns of the fresh and reacted mixture of the sorbent and catalyst/OC after 20 reduction-oxidation-calcination cycles of SE–CLSR are presented in Figure 8. The patterns were identified by the usual peaks of nickel, nickel oxide, alumina and CaO by X'Pert HighScore Plus software for phase analysis of the XRD data. The Scherrer equation was used to find the crystallite size of the Ni/NiO phases. The Ni crystallite sizes of the reacted catalyst were in the range 29.69 – 30.82 nm with no significant difference to those of the C-SR process when compared at same conditions. The NiO crystallite sizes of the fresh and reacted catalyst after the last (20^{th}) oxidation cycle step were in the range 45.1 – 49.1 nm. This represents a significant sintering effect owing to the mixing of the catalyst and sorbent. The effect of reacting temperature was not apparent in the XRD data. A very small peak of Al_2O_3 around 30° 2θ roughly appeared in the reacted catalyst but was absent in the fresh and H_2 reduced catalyst in Figure 8(a) of the SE-SR process system. This might be caused by crystallisation after long (1 hour 30 minutes roughly) exposure of the sorbent and catalyst mixture to reaction temperature. A slight negligible increase in the crystallite size of the reacted mixture of the catalyst/OC was observed. The slight increase could depict sintering of the Ni crystallite during stability test of the catalyst/OC [63]. The great characteristic peaks of NiO matching exactly those of the fresh sorbent and the catalyst/OC mixture suggested sufficient oxidation of the Ni to NiO.

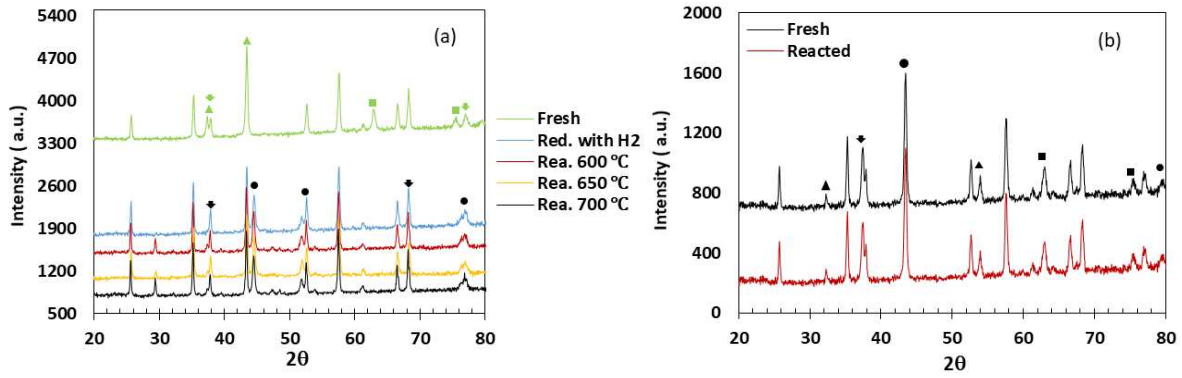

Figure 8 18 wt. % NiO on Al_2O_3 support XRD patterns; triangles are CaO peaks, squares are NiO peaks, arrows are superimposed NiO, CaO and Al_2O_3 peaks, circles represent superimposed NiO and Al_2O_3 peaks, while the unidentified peaks are Al_2O_3 peaks in both processes (a) for SE-SR process, (b) for SE-CLSR process,

Field emission- scanning electron microscopy (FESEM) was used to study morphological characteristics of the sorbent and catalyst/OC. Comparison of the fresh and the reacted CaO sorbent and catalyst/OC mixture after 20 reduction-calcination-oxidation cycles shows sintering and excessive agglomeration of the mixture (see SD8). Expansion of the CaO sorbent particles during CO_2 adsorption causes sintering of the particles [46, 64]. The expansion that causes sintering is extremely influenced by temperature and particle separation distance. A high adsorption temperature and shorter distance between two sorbent particles increases the sintering rate during the adsorption process [46]. The latter, shorter distance between two sorbent particles might be the major cause of sintering in the present studies, since the adsorption temperature is moderately low. With the help of EDX (mapping method) it was found that solid carbon deposition on the surface of the sorbent and catalyst/OC mixture (mixed randomly) was not homogeneously distributed during both processes (SE-SR and SE-CLSR process). The lack of homogeneity from carbon deposition could be attributed to the level/position of the catalyst in the bed. It is expected that the topmost (upstream) part of the catalyst will be more prone to solid carbon deposition than the downstream parts.

The textural properties of the sorbent; BET surface area of the fresh and reacted mixture samples are given in Table 5. The BET surface area of the $CaCO_3$ was found to be 0.349 m^2/g, while after calcination to CaO it was 7.121 m^2/g. The BET surface area of CaO increased significantly due release of CO_2 and

other elements present in the $CaCO_3$; causing formation of a highly porous layer with small particles on the surface of CaO sorbent. The BET surface area of the reacted sorbent and catalyst/OC mixture in SE-CLSR (after 20 reduction-calcination-oxidation cycles) and that of sorbent and catalyst mixture in the SE-SR process show a slight decrease compared to the unused mixture of the sorbent and catalyst/OC, which could be owed to sintering and pore blockage particularly after repeated cyclic absorption and desorption cycles [37] in the SE-CLSR process.

The concentration of solid carbon found on the surface of the sorbent and catalyst/OC mixture using CHNS analysis and that of solid carbon in the condensate (from the TOC analysis) was negligible/insignificant in both processes. Thus, it can be concluded that burning off of the solid carbon during the oxidation reaction process at 850 °C was successful. 157 ppm of solid carbon was found in the condensate sample of 20 reduction-oxidation-calcination cycles collectively. The collective small concentration of the solid carbon also made us consider it insignificant. Overall, the effect of temperature on the surface area, carbon concentration on the surface of the catalyst and the condensate was not obvious. The absence of any major difference in the solid carbon concentration on the surface of the catalyst during SE-SR process was not surprising because all the temperatures were investigated at S:C 3, which thermodynamically inhibits solid carbon deposition [9, 65].

Table 5 Characterisation results after the last (20th) oxidation cycle at 1 bar, GHSV 0.498, S:C 3, reforming/reduction temperature at 650 ℃ and oxidation at ℃ 850 using CaO and Ni on Al_2O_3 support as sorbent and catalyst/OC respectively

Condition	NiO/Ni crystallite size (nm)	BET Surface area (m^2/g)	C (Mole) on catalyst	C (g/L) in condensate
$CaCO_3$	N/A	0.349	N/A	N/A
CaO	48.23	7.121	N/A	N/A
Fresh catalyst	45.05	3.45	N/A	N/A
Reduced catalyst with H_2	30.82	2.256	N/A	N/A
Fresh sorbent and catalyst/OC mixture	44.89	5.131	N/A	N/A
SE-SR Reacted at 600 ℃	29.69	3.060	0.016	0.096
SE-SR Reacted at 650 ℃	30.41	2.532	0.014	0.091
SE-SR Reacted at 700 ℃	30.40	2.901	0.012	0.083

SE-CLSR Reacted at 650 ℃	49.08	4.605	0.001	0.16

5. Conclusion

In order to define the optimum operating conditions for the SE-CLSR process and determine its feasibility with a shale gas feedstock, the effect of Ca based CaO sorbent and operating temperature in the range of 600-700 ℃ was studied first in a packed bed at atmospheric pressure. It was found that low/medium operating temperature is more suitable for a SE-SR process owing to the thermal decomposition of CaO sorbent at high temperatures, in addition to carbonation favoured thermodynamically at low/medium temperatures. However, low operating temperature suppresses catalyst activity. It was also discovered that the presence of CaO as in situ CO_2 sorbent has the potential to decrease operational and capital costs because of milder reactive conditions and lower reactor materials requirements.

High purity H_2 was generated using a novel low energy consumption process termed SE-CLSR process using a gas feedstock closely reproducing an actual shale gas. The feasibility of the intensified C-SR process (coupled with sorption enhancement and chemical looping) was demonstrated experimentally over a mixture of a bifunctional NiO-based catalyst/OC supported on Al_2O_3 and a Ca-based CaO sorbent. 20 reduction-oxidation-calcination cycles of experiments were performed in a bench-scale fixed bed reactor at 1 bar, GHSV 0.498, S:C 3 and 650 ℃. High hydrogen yield of 31 wt. % and purity of 92 % was obtained (in the 4^{th} cycle) during the pre-breakthrough period of the SE-CLSR process (prior to cycles with low sorbent capacity). The post breakthrough period did not degenerate fully to the C-SR process due to catalyst/OC bed dilution with sorbent, and decreased amount of catalyst compared to the C-SR process. The surface area of the sorbent and catalyst/OC mixture after 20 reduction-calcination-oxidation cycles underwent a slight decrease compared fresh mixture of the sorbent and catalyst/OC caused by sintering and pore blockage after repeated cyclic absorption-desorption cycles. The FESEM images of the mixture also showed sintering and agglomeration on the reacted sorbent and catalyst/OC mixture. Sorbent regeneration and Ni oxidation to NiO at 850 ℃

using air feed successfully burned off the solid carbon deposits on the surface of the sorbent and on the catalyst/OC mixture during the oxidation step of SE-CLSR. Regeneration and oxidation of the CaO sorbent and catalyst/OC was also accomplished at the same temperature.

For the process to be commercially applicable, a more advanced analysis and optimisation of the SE-CLSR process is necessary, including, prolonged testing under cyclic conditions, finding mixture conditions of sorbent and catalyst/OC that prevent coking, together with detailed technological and economic analysis and whole process design for scaling purposes. Yet, it is obvious that the combination of sorption enhancement and chemical looping on C-SR process has great prospects for high H_2 yield and purity generation at reasonable lower cost and high energy efficiency.

Acknowledgments

The Petroleum Technology Development Fund (Nigeria) is gratefully acknowledged for the scholarship of Zainab Ibrahim S G Adiya, and we also thank the UKCCSRC EPSRC consortium (EP/K000446/1) for call 2 grant 'Novel Materials and Reforming Process Route for the Production of Ready-Separated CO2/N2/H2 from Natural Gas Feedstocks'. Martyn V. Twigg at TST Ltd is also gratefully acknowledged for providing the nickel-based OC catalyst.

References

[1] Gil MV, Fermoso J, Pevida C, Chen D, Rubiera F. Production of fuel-cell grade H2 by sorption enhanced steam reforming of acetic acid as a model compound of biomass-derived bio-oil. Appl Catal B: Environ. 2016;184:64-76.

[2] Martavaltzi CS, Pampaka EP, Korkakaki ES, Lemonidou AA. Hydrogen production via steam reforming of methane with simultaneous CO2 capture over CaO− Ca12Al14O33. Energ Fuels. 2010;24:2589-95.

[3] De Wilde J, Froment GF. Computational Fluid Dynamics in chemical reactor analysis and design: Application to the ZoneFlow reactor for methane steam reforming. Fuel. 2012;100:48-56.

[4] Wang F, Qi B, Wang G, Li L. Methane steam reforming: Kinetics and modeling over coating catalyst in micro-channel reactor. Int J Hydrogen Energ. 2013;38:5693-704.

[5] Farsi A, Shadravan V, Mansouri SS, Zahedi G, Manan ZA. A new reactor concept for combining oxidative coupling and steam re-forming of methane: modeling and analysis. Int J Energ Res. 2013;37:129-52.

[6] Martínez I, Romano MC, Fernández JR, Chiesa P, Murillo R, Abanades JC. Process design of a hydrogen production plant from natural gas with CO2 capture based on a novel Ca/Cu chemical loop. Appl Energ. 2014;114:192-208.

[7] Collodi G, Wheeler F. Hydrogen Production via Steam Reforming with CO2 Capture. Corsico – Milan - Italy. 2009.

[8] Zhu J, Zhang D, King KD. Reforming of CH4 by partial oxidation: thermodynamic and kinetic analyses. Fuel. 2001;80:899-905.

[9] S G Adiya ZI, Dupont V, Mahmud T. Chemical equilibrium analysis of hydrogen production from shale gas using sorption enhanced chemical looping steam reforming. Fuel Process Technol. 2017;159:128-44.

[10] Anzelmo B, Wilcox J, Liguori S. Natural gas steam reforming reaction at low temperature and pressure conditions for hydrogen production via Pd/PSS membrane reactor. J Membrane Sci. 2017;522:343-50.

[11] Wiranarongkorn K, Arpornwichanop A. Analysis of the Ca-looping sorption-enhanced steam reforming and solid oxide fuel cell integrated process using bio-oil. Energ Convers Manage. 2017;134:156-66.

[12] Spallina V, Marinello B, Gallucci F, Romano MC, Van Sint Annaland M. Chemical looping reforming in packed-bed reactors: Modelling, experimental validation and large-scale reactor design. Fuel Process Technol. 2017;156:156-70.

[13] Hafizi A, Rahimpour MR, Hassanajili S. Hydrogen production via chemical looping steam methane reforming process: Effect of cerium and calcium promoters on the performance of Fe2O3/Al2O3 oxygen carrier. Appl Energ. 2016;165:685-94.

[14] Alirezaei I, Hafizi A, Rahimpour MR. Syngas production in chemical looping reforming process over ZrO2 promoted Mn-based catalyst. J CO2 Util. 2018;23:105–16.

[15] Dou B, Zhang H, Cui G, Wang Z, Jiang B, Wang K, et al. Hydrogen production by sorption-enhanced chemical looping steam reforming of ethanol in an alternating fixed-bed reactor: Sorbent to catalyst ratio dependencies. Energ Convers Manage. 2018;155:243-52.

[16] Balasubramanian B, Ortiz AL, Kaytakoglu S, Harrison D. Hydrogen from methane in a single-step process. Che Eng Sci. 1999;54:3543-52.

[17] Johnsen K, Ryu HJ, Grace JR, Lim CJ. Sorption-enhanced steam reforming of methane in a fluidized bed reactor with dolomite as CO2-acceptor. Che Eng Sci 2006;61: 1195-202.

[18] Speight JG. The chemistry and technology of petroleum Fifth ed. Boca Raton: Taylor and Francis Group, LLC; c2007.

[19] Pérez-Moreno L, Soler J, Herguido J, Menéndez M. Stable hydrogen production by methane steam reforming in a two zone fluidized bed reactor: Experimental assessment. J Power Sources. 2013;243:233-41.

[20] Kumar RV, lyon RK, Cole JA. Unmixed Reforming: A Novel Autothermal Cyclic Steam Reforming Process. US: Springer; 2002.

[21] Kikuchi E. Membrane reactor application to hydrogen production. Catal Tody. 2000;56:97-101.

[22] Matsumura Y, Nakamori T. Steam reforming of methane over nickel catalysts at low reaction temperature. Appl Catal A: General. 2004;258:107-14.

[23] Gallucci F, Paturzo L, Famà A, Basile A. Experimental study of the methane steam reforming reaction in a dense Pd/Ag membrane reactor. Ind eng chem res. 2004;43:928-33.

[24] Chen Y, Wang Y, Xu H, Xiong G. Efficient production of hydrogen from natural gas steam reforming in palladium membrane reactor. Appl Catal B: Environ. 2008;81:283-94.

[25] Tong J, Matsumura Y, Suda H, Haraya K. Experimental study of steam reforming of methane in a thin (6 μM) Pd-based membrane reactor. Ind eng che res. 2005;44:1454-65.

[26] Zheng Y, Li K, Wang H, Tian D, Wang Y, Zhu X, et al. Designed oxygen carriers from macroporous LaFeO3 supported CeO2 for chemical-looping reforming of methane. Appl Catal B: Environ. 2017;202:51-63.

[27] Antzara A, Heracleous E, Silvester L, Bukur DB, Lemonidou AA. Activity study of NiO-based oxygen carriers in chemical looping steam methane reforming. Catal Tody. 2016;272:32-41.

[28] Fan J, Zhu L, Jiang P, Li L, Liu H. Comparative exergy analysis of chemical looping combustion thermally coupled and conventional steam methane reforming for hydrogen production. J Cleaner Production. 2016;131:247-58.

[29] Hafizi A, Rahimpour MR, Hassanajili S. Hydrogen production by chemical looping steam reforming of methane over Mg promoted iron oxygen carrier: Optimization using design of experiments. J Taiwan Institute of Che Eng. 2016;62:140-9.

[30] Lua C, Li K, Wanga H, Zhu X, Wei Y, Zheng M, et al. Chemical looping reforming of methane using magnetite as oxygen carrier: Structure evolution and reduction kinetics Appl Energ 2018;211:1–14.

[31] Aloisi I, Di Giuliano A, Di Carlo A, Foscolo PU, Courson C, Gallucci K. Sorption enhanced catalytic Steam Methane Reforming: Experimental data and simulations describing the behaviour of bi-functional particles. Che Eng J. 2016.

[32] Xu P, Zhou Z, Zhao C, Cheng Z. Catalytic performance of Ni/CaO-Ca5Al6O14 bifunctional catalyst extrudate in sorption-enhanced steam methane reforming. Catal Tody. 2016;259, Part 2:347-53.

[33] Broda M, Manovic V, Imtiaz Q, Kierzkowska AM, Anthony EJ, Müller CR. High-Purity Hydrogen via the Sorption-Enhanced Steam Methane Reforming Reaction over a Synthetic CaO-Based Sorbent and a Ni Catalyst. Environ Sci Technol. 2013;47:6007−14.

[34] Xie M, Zhou Z, Qi Y, Cheng Z, Yuan W. Sorption-enhanced steam methane reforming by in situ CO2 capture on a CaO–Ca9Al6O18 sorbent. Che Eng J. 2012;207–208:142-50.

[35] Fernandez JR, J.C.Abanades, R.Murillo. Modeling of sorption enhanced steam methane reforming in an adiabatic fixed bed reactor. Che Eng Sci. 2012;84:1-11.

[36] Pimenidou P, Rickett G, Dupont V, Twigg MV. High purity H2 by sorption-enhanced chemical looping reforming of waste cooking oil in a packed bed reactor. Bioresource Technol 2010;101:9279–86.

[37] Hafizi A, Rahimpour MR, Hassanajili S. High purity hydrogen production via sorption enhanced chemical looping reforming: Application of 22Fe2O3/MgAl2O4 and 22Fe2O3/Al2O3 as oxygen carriers and cerium promoted CaO as CO2 sorbent. Appl Energ. 2016;169:629-41.

[38] Antzara A, Heracleous E, Lemonidou AA. Energy efficient sorption enhanced-chemical looping methane reforming process for high-purity H2 production: Experimental proof-of-concept. Appl Energ. 2016;180:457-71.

[39] Ryden M, Ramos P. H2 production with CO2 capture by sorption enhanced chemical-looping reforming using NiO as oxygen carrier and CaO as CO_2 sorbent. Fuel Process Technol. 2012;96:27-36.

[40] Fan J, Zhu L. Performance analysis of a feasible technology for power and high-purity hydrogen production driven by methane fuel. Appl Therm Eng. 2015;75:103-14.

[41] Zhu L, Fan J. Thermodynamic analysis of H2 production from CaO sorption-enhanced methane steam reforming thermally coupled with chemical looping combustion as a novel technology. Int J Energy Res. 2015;39:356–69.

[42] Fernandez JR, Abanades JC, Grasa G. Modeling of sorption enhanced steam methane reforming—Part II: Simulation within a novel Ca/Cu chemical loop process for hydrogen production. Che Eng Sci. 2012;84:12-20.

[43] S G Adiya ZI, Dupont V, Mahmud T. Effect of hydrocarbon fractions, N2 and CO2 in feed gas on hydrogen production using sorption enhanced steam reforming: Thermodynamic analysis. Int J Hydrogen Energ. 2017;42:21704-18.

[44] Udengaard NR. Hydrogen production by steam reforming of hydrocarbons. Preprint Papers-American Chemical Society, Division of Fuel Chemistry. 2004;49:906-7.

[45] Abbas SZ, Dupont V, Mahmud T. Kinetics study and modelling of steam methane reforming process over a NiO/Al2O3 catalyst in an adiabatic packed bed reactor. Int J Hydrogen Energ. 2016;42:2889–903.

[46] Shokrollahi Yancheshmeh M, Radfarnia HR, Iliuta MC. High temperature CO2 sorbents and their application for hydrogen production by sorption enhanced steam reforming process. Che Eng J. 2016;283:420-44.

[47] S G Adiya ZI, Dupont V, Mahmud T. Steam reforming of shale gas in a packed bed reactor with and without chemical looping using nickel based oxygen carrier. Int J Hydrogen Energy 2018;43: 6904-17.

[48] Bullin K, Krouskop P. Composition variety complicates processing plans for US shale gas. USA: Bryan Research & Engineering, Inc; 2008.

[49] Florin NH, Harris AT. Hydrogen production from biomass coupled with carbon dioxide capture: The implications of thermodynamic equilibrium. Int J Hydrogen Energy. 2007;32:4119-34.

[50] Wei L, Xu S, Liu J, Liu C, Liu S. Hydrogen Production in Steam Gasification of Biomass with CaO as a CO2 Absorbent. Energy Fuels. 2004;22:1997–2004.

[51] Wang X, Wang N, Wang L. Hydrogen production by sorption enhanced steam reforming of propane : A thermodynamic investigation. Int J Hydrogen Energy. 2011;36:466-72.

[52] Antzara A, Heracleous E, Bukur DB, Lemonidou AA. Thermodynamic analysis of hydrogen production via chemical looping steam methane reforming coupled with in situ CO2 capture. Inte J Greenhouse Gas Control. 2015;32:115-28.

[53] Ding Y, Alpay E. Adsorption enhanced steam-methane reforming. Che Eng Sci. 2000;55:3929-40.

[54] Martavaltzi CS, Lemonidou AA. Hydrogen production via sorption enhanced reforming of methane: Development of a novel hybrid material—reforming catalyst and CO2 sorbent. Che Eng Sci. 2010;65:4134-40.

[55] Zin RM, Lea-Langton A, Dupont V, Twigg MV. High hydrogen yield and purity from palm empty fruit bunch and pine pyrolysis oils. Int J Hydrogen Energ. 2012;37:10627-38.

[56] Esteban-Díez G, Gil MV, Pevida C, Chen D, Rubiera F. Effect of operating conditions on the sorption enhanced steam reforming of blends of acetic acid and acetone as bio-oil model compounds. Appl Energ. 2016;177:579-90.

[57] Albrecht KO, Satrio JA, Shanks BH, Wheelock TD. Application of a combined catalyst and sorbent for steam reforming of methane. Ind Eng Che Res. 2010;49:4091-8.

[58] Silaban A, Narcida M, Harrison D. Characteristics of the reversible reaction between CO2 (g) and calcined dolomite. Che Eng Commun. 1996;146:149-62.

[59] Sun P, Lim CJ, Grace JR. Cyclic CO2 capture by limestone-derived sorbent during prolonged calcination/carbonation cycling. AIChe Journal. 2008;54:1668-77.

[60] Fennell P, Anthony B. Calcium and Chemical Looping Technology for Power Generation and Carbon Dioxide (CO2) Capture: Elsevier; 2015.

[61] Rydén M, Johansson M, Lyngfelt A, Mattisson T. NiO supported on Mg–ZrO 2 as oxygen carrier for chemical-looping combustion and chemical-looping reforming. Energ Environ Sci. 2009;2:970-81.

[62] Grasa GS, Abanades JC. CO2 capture capacity of CaO in long series of carbonation/calcination cycles. Ind Eng Che Res. 2006;45:8846-51.

[63] Wang K, Dou B, Jiang B, Zhang Q, Li M, Chen H, et al. Effect of support on hydrogen production from chemical looping steam reforming of ethanol over Ni-based oxygen carriers. Int J Hydrogen Energ. 2016;41:17334-47.

[64] Zhang L, Lu Y, Rostam-Abadi M. Sintering of calcium oxide (CaO) during CO 2 chemisorption: a reactive molecular dynamics study. Phys Chem. 2012;14:16633-43.

[65] Dupont V, Twigg MV, Rollinson AN, Jones JM. Thermodynamics of hydrogen production from urea by steam reforming with and without in situ carbon dioxide sorption. Int J Hydrogen Energy. 2013;38:10260-9.